Downloaded from UvA-DARE, the institutional repository of the University of Amsterdam (UvA)
http://hdl.handle.net/11245/2.30132

File ID uvapub:30132
Filename 135862y.pdf
Version unknown

SOURCE (OR PART OF THE FOLLOWING SOURCE):
Type article
Title The dynamics of a hole in a CuO4 plaquette: electron energy-loss spectroscopy of Li2CuO2
Author(s) S. Atzkern, M. Knupfer, M.S. Golden, J. Fink, C. Waidacher, J. Richter, K.W. Becker, N. Motoyama, H. Eisaki
Faculty UvA: Universiteitsbibliotheek
Year 2000

FULL BIBLIOGRAPHIC DETAILS:
http://hdl.handle.net/11245/1.423964

Copyright

It is not permitted to download or to forward/distribute the text or part of it without the consent of the author(s) and/or copyright holder(s), other than for strictly personal, individual use, unless the work is under an open content licence (like Creative Commons).

UvA-DARE is a service provided by the library of the University of Amsterdam (http://dare.uva.nl)
(pagedate: 2014-11-27)

Dynamics of a hole in a CuO_4 plaquette: Electron energy-loss spectroscopy of Li_2CuO_2

S. Atzkern, M. Knupfer, M. S. Golden, and J. Fink
Institut für Festkörper- und Werkstofforschung Dresden, P.O. Box 270016, D-01171 Dresden, Germany

C. Waidacher, J. Richter, and K. W. Becker
Institut für Theoretische Physik, Technische Universität Dresden, D-01062 Dresden, Germany

N. Motoyama, H. Eisaki, and S. Uchida
Department of Superconductivity, The University of Tokyo, Bunkyo-ku, Tokyo 113, Japan
(Received 26 January 2000)

We have measured the energy- and momentum-dependent loss function of Li_2CuO_2 single crystals by means of electron energy-loss spectroscopy in transmission. Using the same values for the model parameters, the low-energy features of the spectrum as well as published Cu $2p_{3/2}$ x-ray photoemission data of Li_2CuO_2 are well described by a cluster model that consists of a single CuO_4 plaquette only. This demonstrates that charge excitations in Li_2CuO_2 are strongly localized.

I. INTRODUCTION

At present, a large variety of cuprate compounds with different element compositions and various crystal structures are known. The common structural unit of nearly all these materials is the square planar CuO_4 plaquette with the oxygen atoms at the corners and the copper atom in the center. The CuO_4 plaquettes can share oxygen atoms with their nearest-neighbor plaquettes, thus building chains or planes. These Cu-O networks are separated generally by counterions. Therefore, the electronic properties of the cuprates are low-dimensional.

For a given doping level, the arrangement of the plaquettes in the crystal is decisive in determining the mobility and correlation of the charge carriers. Therefore, it influences the particular physical properties of the cuprate compound under consideration. For instance, in many two-dimensional (2D) systems, high-T_c superconductivity can be observed and among the quasi-one-dimensional (1D) cuprates there exist excellent candidates for studying typically one-dimensional properties. Examples are the spin-Peierls transition which occurs in edge-sharing chains ($CuGeO_3$) (Ref. 1) or spin-charge separation in corner-sharing chains (Sr_2CuO_3).[2–4] Furthermore, in the spin ladder compounds the ordering of the CuO_4 plaquettes lies between 1D and 2D. Their magnetic properties change discontinuously with the transition from 1D to 2D.[5] One example of such a system is $Sr_{0.4}Ca_{13.6}Cu_{24}O_{41}$, which consists of two-leg ladders as well as chains of edge-sharing plaquettes in alternating layers and which shows superconductivity under high pressure (3 GPa).[6]

In the hole picture (in the undoped case) every CuO_4 plaquette is occupied by a single hole in otherwise empty Cu $3d$ and O $2p$ orbitals. Thus, in the case of interconnected CuO_4 plaquettes the theoretical analysis of the electronic structure has to deal with many-particle systems, and the interpretation of corresponding experimental data is rather complex. Furthermore, it is usually not possible to determine all theoretical model parameters for the Cu-O network from experiments. For these reasons it is helpful to study in detail the electronic properties of the structural unit itself, a single plaquette, to establish a basis for all Cu-O networks.

On the other hand, in real materials, plaquettes are never truly isolated. Therefore, we have to choose a system in which the electronic interaction between the holes on the plaquettes and charge carriers in their vicinity can be estimated to be small. One candidate for such a system is Li_2CuO_2. In view of the structure of Li_2CuO_2 (see Fig. 1), one might assign this compound to the 1D systems due to the parallel aligned chains of edge-sharing plaquettes. However, since the Cu-O-Cu-bond angle along the chains is almost 90°, the hopping from one plaquette to its nearest neighbor is strongly suppressed. Thus, although the magnetic interactions in Li_2CuO_2 are rather complex,[7–10] with respect to the electronic properties the plaquettes in this compound can be considered as approximately isolated.

Recently, the optical properties and the electronic struc-

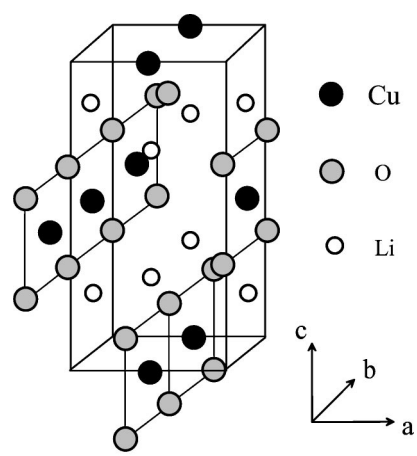

FIG. 1. Crystal structure of Li_2CuO_2. The Cu atoms (black filled circles) and their nearest neighbor O atoms (gray filled circles) build chains of edge sharing CuO_4 plaquettes along **b**. The Li atoms (open circles) are located right below and above the Cu atoms in the **c** direction.

 ©2000 The American Physical Society

ture of Li_2CuO_2 have been studied carrying out reflectivity,[11] x-ray photoemission,[14] and x-ray absorption[15] measurements. In this paper, we present transmission electron energy-loss spectroscopy (EELS) studies of Li_2CuO_2. The resulting spectra allow us to study the multipole transitions between the ground state and the excited states of an approximately isolated single plaquette. Our theoretical analysis shows that the EELS results, as well as the Cu $2p_{3/2}$ x-ray photoemission spectrum published by Böske *et al.*,[14] can be described in a multiband Hubbard model using the same parameter values for the charge-transfer energy and the hopping amplitudes.

II. EXPERIMENT

Single crystals of Li_2CuO_2 were grown using a traveling solvent-zone technique.[11] The crystal structure is shown in Fig. 1. Li_2CuO_2 has a body-centered orthorhombic unit cell (space-group *Immm*) with the lattice constants $a=3.661$ Å, $b=2.863$ Å, and $c=9.393$ Å. Edge-sharing CuO_4 plaquettes lie in the (**a**,**b**) plane and the chains are aligned along the **b** direction.[16,17] The Cu-O distance within the plaquette is 1.958 Å while the O-O distances in the **b** and **c** direction are 2.863 Å and 2.671 Å, respectively. This configuration implies a Cu-O-Cu bond angle of about 94°. The distances between a Cu atom in one chain and O atoms of neighboring chains are larger than 3 Å. This suggests that the electronic interchain coupling is small.

Electron energy-loss spectroscopy (EELS) in transmission was performed on free-standing films of about 1000 Å thickness which were cut from the crystals using an ultramicrotome with a diamond knife. All measurements were carried out at room temperature and with a momentum transfer parallel to the **b** and **c** axis. The primary beam energy was 170 keV. The energy resolution ΔE and the momentum transfer resolution Δq were chosen to be 110 meV and 0.05 Å^{-1} for $q \leqslant 0.4$ Å^{-1}, and 160 meV and 0.06 Å^{-1} for $q > 0.4$ Å^{-1}.

EELS provides us with the energy and momentum dependent loss function $\mathrm{Im}(-1/\varepsilon(\omega,\mathbf{q}))$ which is directly proportional to the imaginary part of the dynamical density-density correlation function

$$\chi_\rho(\omega,\mathbf{q}) = \frac{1}{i}\int_0^\infty dt e^{-i\omega t}\langle\Psi|[\rho_{-\mathbf{q}}(0),\rho_{\mathbf{q}}(t)]|\Psi\rangle. \qquad (1)$$

$|\Psi\rangle$ describes the ground state of the Hamiltonian and $\rho_{\mathbf{q}}$ is the Fourier-transformed hole density (see below). Equation (1) implies that for the limit $\mathbf{q}\to 0$ the selection rules for transitions are the same as in optics, i.e., dipole transitions are allowed. For finite **q**, nondipole transitions additionally contribute to the loss function.

III. RESULTS AND DISCUSSION

In Fig. 2 we show the loss function as well as the real part of the dielectric function, ε_1, and the optical conductivity, $\sigma=\omega\varepsilon_0\varepsilon_2$, of Li_2CuO_2 for a momentum transfer of $\mathbf{q}=0.08$ Å^{-1}. The latter two have been derived by a Kramers-Kronig analysis. The loss function is dominated by a broad feature around 21 eV, which represents the volume plasmon, a collective excitation of all valence electrons. At lower energies, several further plasmon excitations can be observed which are related to transitions between occupied and unoccupied electronic states with mainly Cu $3d$, Cu $4s$, and O $2p$ character. These transitions give rise to the maxima in the optical conductivity, which is shown in the lower panel of Fig. 2. At small momentum transfers, σ as derived from EELS can be directly compared to results from optical measurements. The optical conductivity of Li_2CuO_2 shown in Fig. 2 is in good agreement with recent optical studies.[11] Note that the corresponding maxima in the loss function are observed at higher energies when compared to the optical conductivity. This is a direct consequence of the collective nature of the plasmon excitations as observed in the loss function.[18]

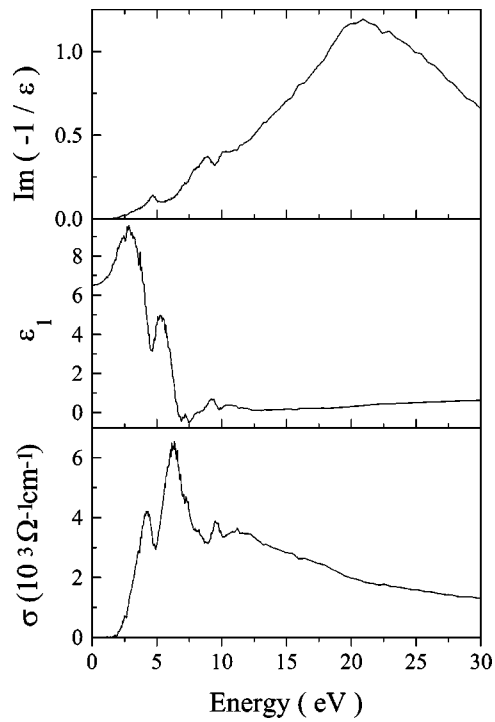

FIG. 2. Loss function, $\mathrm{Im}(-1/\varepsilon)$ (upper panel), real part of the dielectric function, ε_1 (middle panel), and optical conductivity, $\sigma=\omega\varepsilon_0\varepsilon_2$ (lower panel) of Li_2CuO_2 for a small momentum transfer of 0.08 Å^{-1} along the **b** direction.

Figure 3(a) focuses on the loss function in a smaller energy range as a function of the momentum transfer. For small momentum transfer the energy range up to 6 eV is dominated by one distinct peak at 4.7 eV. With increasing **q** the intensity of this peak decreases while the intensity of a second feature around 5.7 eV, which becomes visible at $q \geqslant 0.7$ Å^{-1}, increases. This behavior of the two features can be explained by the different multipole character of the corresponding transitions (see below). The steep rise of the background above 6 eV is due to the higher-lying excitations (see Fig. 2).

Since the Cu-O-Cu bond angle is close to 90°, the nearest-neighbor (NN) Cu-O-Cu hopping amplitude is small, and the delocalization properties of the system are dominated by a weak next-nearest-neighbor (NNN) Cu-O-O-Cu hopping.[7] In the loss function, the NN as well as the NNN hopping might be visible in the tail of nonvanishing spectral weight between the spectral onset at $\sim$1.5 eV and the main

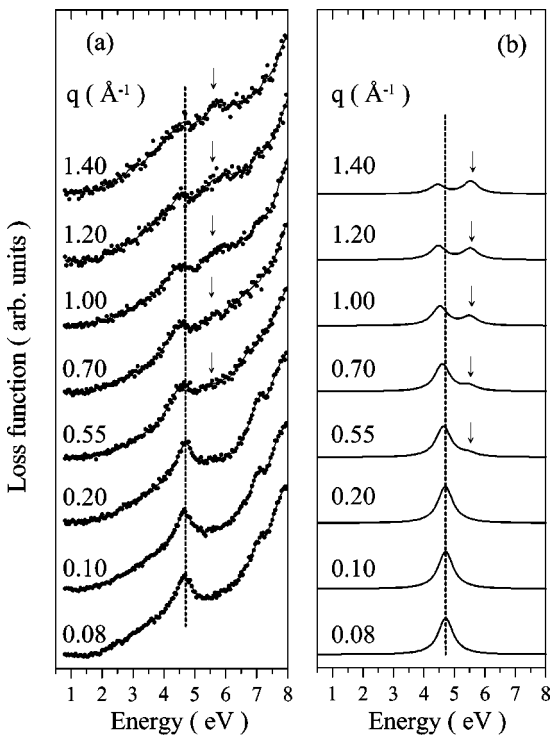

FIG. 3. Loss function of Li_2CuO_2 (left panel) measured with different momentum transfers **q** parallel to the chain direction. The right panel shows the calculated dynamical density-density correlation function for the same **q** values. The vertical dashed lines and the arrows illustrate the small dispersion of the main peak and the increase of spectral weight with increasing **q** around 5.5 eV, respectively.

peak at 4.5 eV, as has been discussed previously.[11] However, in a first approximation the CuO_4 plaquettes can be regarded as isolated and the charge excitations in the Cu-O network of Li_2CuO_2 as localized. This is supported by the small dispersion of the features in the EELS spectra, which is in contrast to the strong positive dispersion of about 0.5 eV of the lowest-lying excitations, e.g., in the 1D system Sr_2CuO_3 (Ref. 4) and in the 2D system $Sr_2CuO_2Cl_2$.[12,13] In addition, the fact that the spectra for **q** parallel to the **c** direction (not shown) are essentially identical to those for **q** parallel to the **b** direction also demonstrates the zero-dimensional character of the excitations.

Consequently, our model system for the calculation of the loss functions consists of a single CuO_4 plaquette only. This is a cluster with one Cu $3d_{x^2-y^2}$ orbital and four O $2p_{x(y)}$ orbitals (with site index $j=1,\ldots,4$), which is occupied by a single hole. The restriction to solely these orbitals is fully consistent with x-ray absorption measurements which indicate that the highest occupied states in Li_2CuO_2 have only small hole density in orbitals perpendicular to the CuO_4 plaquette.[15] In this case, $\rho_{\mathbf{q}}$ has the form

$$\rho_{\mathbf{q}}=n^d+\sum_j n_j^p e^{i\mathbf{q}\cdot\mathbf{r}_j} \tag{2}$$

and the Hamiltonian reads

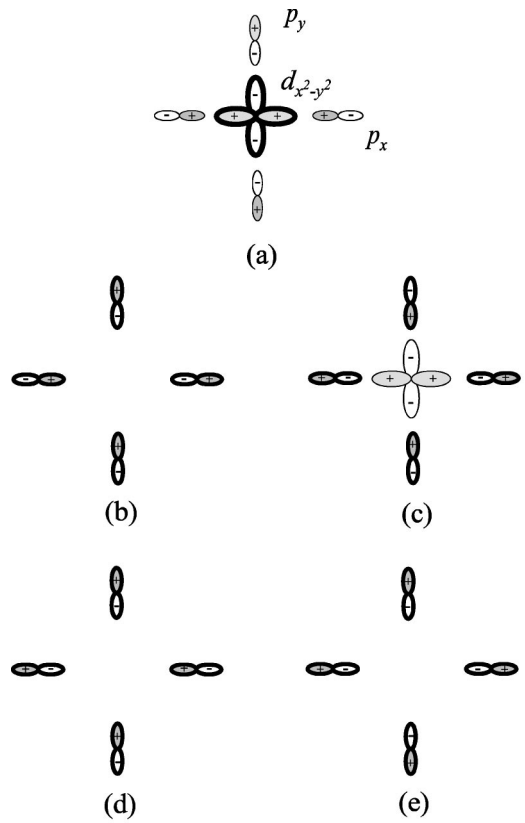

FIG. 4. Symmetry properties of the ground state (a) and the final states (b)–(e) of Hamiltonian (3). The relevant combinations of the hole occupied orbitals (Cu $3d_{x^2-y^2}$ and O $2p_{x,y}$) in the plaquette are shown. Thicker lines correspond to larger hole densities. The states (b), (d), and (e) have zero Cu weight. For momentum transfer parallel to the chain direction, nonvanishing contributions come only from the final states (b) and (c).

$$H=\Delta\sum_j n_j^p+t_{pd}\sum_j \phi_j(p_j^\dagger d+d^\dagger p_j)+t_{pp}\sum_{\langle j,j'\rangle}\phi_{jj'}p_{j'}^\dagger p_j. \tag{3}$$

$d^\dagger$ ($p_j^\dagger$) creates a hole in the Cu $3d$ orbital (jth O $2p$ orbital), with occupation number operators n^d (n_j^p). Δ is the charge-transfer energy. There are two hopping parameters: t_{pd} for the Cu-O hopping and t_{pp} for the O-O hopping. The signs for the hopping are defined as follows: $\phi_1=\phi_2=-1$, $\phi_3=\phi_4=1$, and $\phi_{jj'}=-\phi_j\phi_{j'}$. $\langle jj'\rangle$ denotes the summation over nearest neighbor pairs. Hamiltonian (3) is the simplest model which captures the essential features of the system. It can easily be solved exactly. The inclusion of anisotropic hopping will be discussed below.

Figure 4 shows the symmetry properties of the ground state (a) and the four excited states (b)–(e) of model (3). The ground state is a σ-bonding combination of the Cu $3d_{x^2-y^2}$ orbital and the four O $2p$ orbitals. Transitions into states (c) and (e) are optically forbidden. Thus, they only contribute to the loss function for finite momentum transfer. Moreover, if **q** is parallel to the chain direction, nonvanishing contributions arise only from transitions into the final states (b) and (c). State (b) has pure O $2p$ character, whereas state (c) is the antibonding counterpart to (a). For $\mathbf{q}=\mathbf{0}$, dipole transitions into state (b) lead to spectral weight at energy ω_1. A second

excitation at energy ω_2 due to transitions into state (c) has nonvanishing weight for $\mathbf{q}\neq\mathbf{0}$:

$$\omega_1=\frac{\Delta+2t_{pp}+\omega_2}{2}, \tag{4}$$

$$\omega_2=\sqrt{(\Delta-2t_{pp})^2+16t_{pd}^2}. \tag{5}$$

These transitions, with energies ω_1 and ω_2, appear as plasmon excitations in the EELS spectra at somewhat higher energies ω_1^{RPA} and ω_2^{RPA}. This effect is a result of the long-range Coulomb interaction (see also the discussion above). In the theoretical model this issue can be satisfactorily treated within the random-phase approximation (RPA).[19]

From the experimental spectrum we obtain for small momentum transfer $\omega_1^{\mathrm{RPA}}=4.7$ eV [see Fig. 3(a)]. For larger **q** the experimental spectra show first a small negative dispersion of the main peak [see the deviation from the vertical dashed line in Fig. 3(a)] amounting to about 0.3 eV in the range between 0.1 and 1.4 Å $^{-1}$. This can be assigned to the decrease of the long-range Coulomb potential and the decreasing oscillator strength of the transition with increasing **q**. Second, the spectral weight between 5.5 and 5.8 eV [in Fig. 3(a) marked by arrows] is enhanced at higher **q**, resulting from the plasmon excitation related to the dipole-forbidden transition at ω_2. Since the excitation into the final state (c) corresponds to an octupole transition, the intensity of the corresponding feature in the EELS spectra is low at small **q**, and becomes visible only at rather high momentum transfers.

The two excitation energies ω_1 and ω_2 in Eqs. (4) and (5) are described by the charge-transfer energy Δ and the two hopping parameters t_{pd} and t_{pp}. Thus the energy positions of the two peaks observed in the EELS spectra do not yet determine the parameter set in a unique way. In order to remove the last degree of freedom in our model, we use experimental evidence from Cu $2p_{3/2}$ core-level x-ray photoemission spectroscopy (XPS). Thereby, we take advantage of the fact that three additional measured parameters in the XPS spectra, namely the energy positions as well as the ratio of the spectral weights of the main and satellite line, are obtained, whereas only two variables are added to our model, namely the Coulomb repulsion U_{dc} and the exchange parameter I_{dc}. As explained in Ref. 20 for other compounds, we use model (3) to calculate the core-level XPS of Li_2CuO_2. Good agreement with the experimental spectra[14] is obtained if $t_{pd}^2/(\Delta-2t_{pp})$ lies between 0.7 and 0.8 eV.

It turns out that both the EELS and the XPS results can be described using one single parameter set for Hamiltonian (3): $\Delta=2.7$ eV, $t_{pd}=1.25$ eV, and $t_{pp}=0.32$ eV,[21] which thus represents the most reliable parameter values for a CuO_4 plaquette in Li_2CuO_2. Our values for the charge-transfer energy Δ and the O-O hopping t_{pp} lie between those obtained from band-structure calculations[7] ($\Delta=2.5$ eV, $t_{pp}=0.25$ eV), and from a fit to optical measurements[11] ($\Delta=3.2$ eV, $t_{pp}=0.56$ eV), while the value for t_{pd} is about 10% larger than in Refs. 7 and 11.

In Figs. 3(b) and 5 the theoretical results are compared to the experimental EELS and XPS spectra. The theoretical spectra have been artificially broadened with a full width at half maximum of 0.6 eV for the EELS [Fig. 3(b)] and 1.8 eV

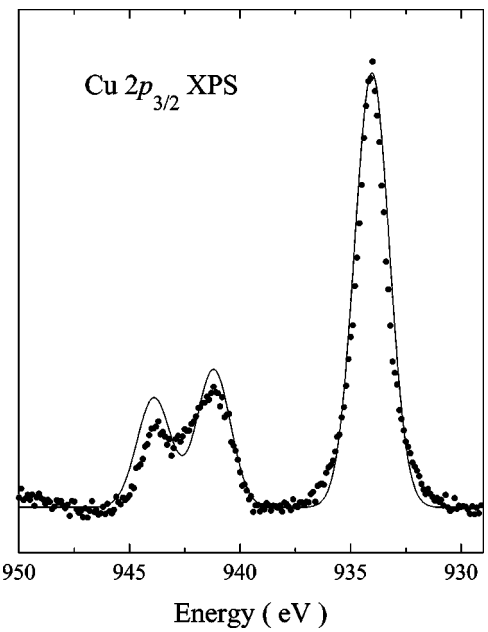

FIG. 5. Cu $2p_{3/2}$ photoemission spectrum of Li_2CuO_2, taken from Ref. 14. The solid line shows the theoretical results. Details of the calculation are described in Ref. 20.

for the XPS (Fig. 5). In agreement with the experimental result [Fig. 3(a)], the calculated EELS data for small momentum transfer consist of a single peak at $\omega_1^{\mathrm{RPA}}=4.7$ eV. The energy $\omega_1=4.4$ eV, calculated with the parameter set received from our data, agrees well with the peak position in the optical conductivity as obtained performing a Kramers-Kronig analysis (see Fig. 2) and as derived from optical studies.[11] For increasing momentum transfer, the peak in the calculated loss function shows a small negative dispersion which is also in full agreement with the experiment. Furthermore, a second feature appears around $\omega_2^{\mathrm{RPA}}=5.5$ eV; the symmetry properties of the associated final states have been discussed above. As regards the XPS results (Fig. 5), we also find a good agreement between theory and experiment. The structure of the experimental spectrum, which consists of a broad satellite (at higher binding energies) and a narrow main line, is correctly reproduced. In addition, the theoretical value for the ratio of the spectral weights of the satellite and the main line coincides with the experimental intensity ratio (0.56).[14]

We conclude with a short discussion of anisotropic hopping. In Li_2CuO_2, the O-O distance in the chain direction (**b** direction) is about 7% larger than in the **c** direction.[17] Thus, one expects an anisotropy in the O-O hopping, with a larger hopping parameter $t_{pp}^{\perp}$ perpendicular to the chain direction (see also Ref. 11). However, if **q** is parallel to the chain direction, a larger $t_{pp}^{\perp}$ in the present model can be absorbed into a renormalized charge-transfer energy Δ without affecting the spectra. As the anisotropy of the edge-sharing CuO_4 plaquettes results in a finite Cu-O-Cu hopping to the next CuO_4 unit, an increase of this anisotropy causes a step towards a one-dimensional electronic system. This is actually realized in the related spin-Peierls compound $CuGeO_3$ where the anisotropy is about 16%. Thus, $CuGeO_3$ might be an ideal candidate for the investigation of the electronic structure of a system at the border to one dimension.

IV. SUMMARY

In summary, we have carried out EELS measurements of Li_2CuO_2 single crystals. Using the same model with the same parameter values, calculations of the energy- and momentum-dependent loss function of an isolated CuO_4 plaquette as well as of the Cu $2p_{3/2}$ core-level XPS of Li_2CuO_2 agree well with the experimentally observed low-energy features of EELS as well as with published XPS data, respectively. Thus, a single parameter set for the charge-transfer energy ($\Delta = 2.7$ eV), the copper-oxygen ($t_{pd} = 1.25$ eV), and oxygen-oxygen ($t_{pp} = 0.32$ eV) hopping amplitudes is sufficient to describe two independent experiments probing the electronic structure of Li_2CuO_2 in completely different energy ranges. These results confirm the strongly localized character of charge excitations in Li_2CuO_2.

ACKNOWLEDGMENT

This work was supported by DFG through the research program of the SFB 463, Dresden.

[1] M. Hase, I. Terasaki, and K. Uchinokura, Phys. Rev. Lett. **70**, 3651 (1993).
[2] E.H. Lieb and F.Y. Wu, Phys. Rev. Lett. **20**, 1445 (1968).
[3] H. Fujisawa, T. Yokoya, T. Takahashi, S. Miyasaka, M. Kibune, and H. Takagi, Phys. Rev. B **59**, 7358 (1999).
[4] R. Neudert, M. Knupfer, M.S. Golden, J. Fink, W. Stephan, K. Penc, N. Motoyama, H. Eisaki, and S. Uchida, Phys. Rev. Lett. **81**, 657 (1998).
[5] E. Dagotto and T.M. Rice, Science **271**, 618 (1996).
[6] M. Uehara, T. Nagata, J. Akimitsu, H. Takahashi, N. Mori, and K. Kinoshita, J. Phys. Soc. Jpn. **65**, 2764 (1996).
[7] R. Weht and W.E. Pickett, Phys. Rev. Lett. **81**, 2502 (1998).
[8] M. Boehm, S. Coad, B. Roessli, A. Zheludev, M. Zolliker, P. Böni, D. McK. Paul, H. Eisaki, N. Motoyama, and S. Uchida, Europhys. Lett. **43**, 77 (1998).
[9] V.Yu. Yushankhai and R. Hayn, Europhys. Lett. **47**, 116 (1999).
[10] Y. Mizuno, T. Tohyama, and S. Maekawa, Phys. Rev. B **60**, 6230 (1999).
[11] Y. Mizuno, T. Tohyama, S. Maekawa, T. Osafune, N. Motoyama, H. Eisaki, and S. Uchida, Phys. Rev. B **57**, 5326 (1998).
[12] Y. Y. Wang, F. C. Zhang, V. P. Dravid, K. K. Ng, M. V. Klein, S. E. Schnatterly, and L. L. Miller, Phys. Rev. Lett. **77**, 1809 (1996).
[13] R. Neudert, T. Böske, O. Knauff, M. Knupfer, M.S. Golden, G. Krabbes, J. Fink, H. Eisaki, and S. Uchida, Physica B **230-232**, 847 (1997).
[14] T. Böske, K. Maiti, O. Knauff, K. Ruck, M.S. Golden, G. Krabbes, J. Fink, T. Osafune, N. Motoyama, H. Eisaki, and S. Uchida, Phys. Rev. B **57**, 138 (1998).
[15] R. Neudert, H. Rosner, S.-L. Drechsler, M. Kielwein, M. Sing, Z. Hu, M. Knupfer, M.S. Golden, J. Fink, N. Nücker, M. Merz, S. Schuppler, N. Motoyama, H. Eisaki, S. Uchida, M. Domke, and G. Kaindl, Phys. Rev. B **60**, 13 413 (1999).
[16] R. Hoppe and H. Riek, Z. Anorg. Allg. Chem. **379**, 157 (1970).
[17] F. Sapiña, J. Rodriguez-Carvajal, M.J. Sanchis, R. Ibañez, A. Beltrán, and D. Beltrán, Solid State Commun. **74**, 779 (1990).
[18] J. Fink, Adv. Electron. Electron Phys. **75**, 121 (1989).
[19] See, e.g., D. Pines, *Elementary Excitations in Solids* (Addison-Wesley, Reading, MA, 1963), Chaps. 3 and 4.
[20] C. Waidacher, J. Richter, and K. W. Becker, Europhys. Lett. **47**, 77 (1999).
[21] The influence of the core hole in the XPS has been modeled using a Coulomb repulsion $U_{dc} = 8.35$ eV and an exchange parameter $I_{dc} = -1.5$ eV, consistent with other cuprates (see Ref. 20).